CellPress

Supplemental figures

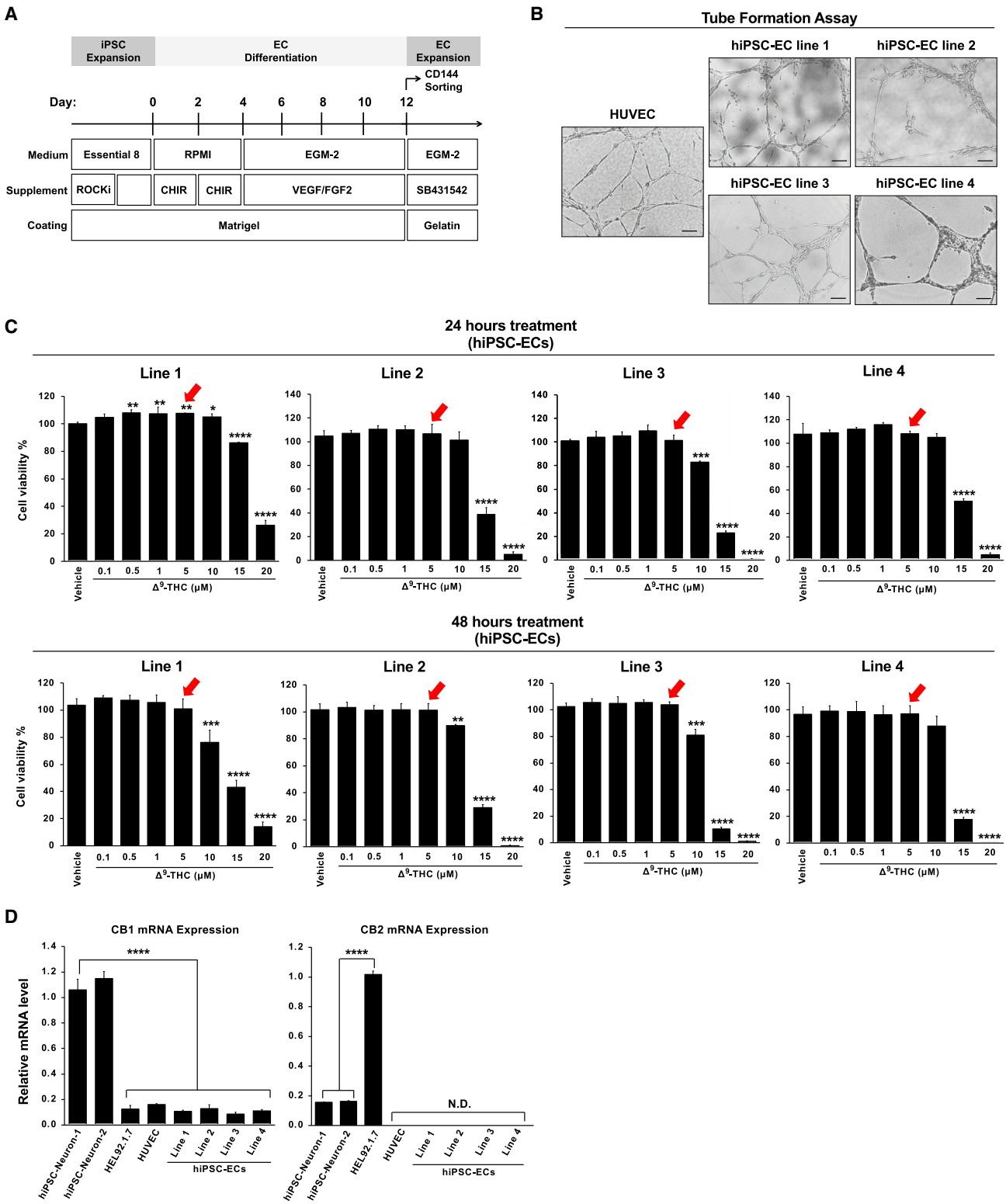

(legend on next page)

Figure S1. Assessment of the effects of Δ^9-THC on cytotoxicity in hiPSC-ECs, related to Figure 3

(A) Endothelial cell differentiation protocol by sequential administration of chemicals and growth factors. Initially, hiPSC differentiation was blocked with a 5 μM Rho kinase inhibitor (ROCKi). When hiPSCs were 80% confluent, differentiation to cardiac mesoderm was facilitated with 6 μM small molecule inhibitor CHIR99021 (CHIR). On day 2, CHIR concentration was reduced to 2 μM. Cells were differentiated to hiPSC-ECs by transitioning from RPMI to EGM2 media with the addition of vascular endothelial growth factor (VEGF) (25 ng/mL), fibroblast growth factor (FGF2) (8 ng/mL), and the small molecule transcription growth factor β1 inhibitor (SB431542) (10 μM).

(B) hiPSC-ECs formed tube-like structures on Matrigel (scale bar, 50 μm).

(C) Cells were treated with various concentrations of Δ^9-THC for 24 or 48 h, and the CellTiter-Glo luminescent cell viability assay measured cell viability. The red arrowhead indicates the concentration used in this study.

(D) CB1 and CB2 expression levels in various cells were measured by qPCR analysis and normalized to GAPDH. Error bars represent mean ± SEM. *$p < 0.05$ versus vehicle; **$p < 0.01$ versus vehicle; ***$p < 0.001$ versus vehicle; ****$p < 0.0001$ versus vehicle; ns, not significant versus vehicle; N.D., not detected for 40 cycles by qPCR.

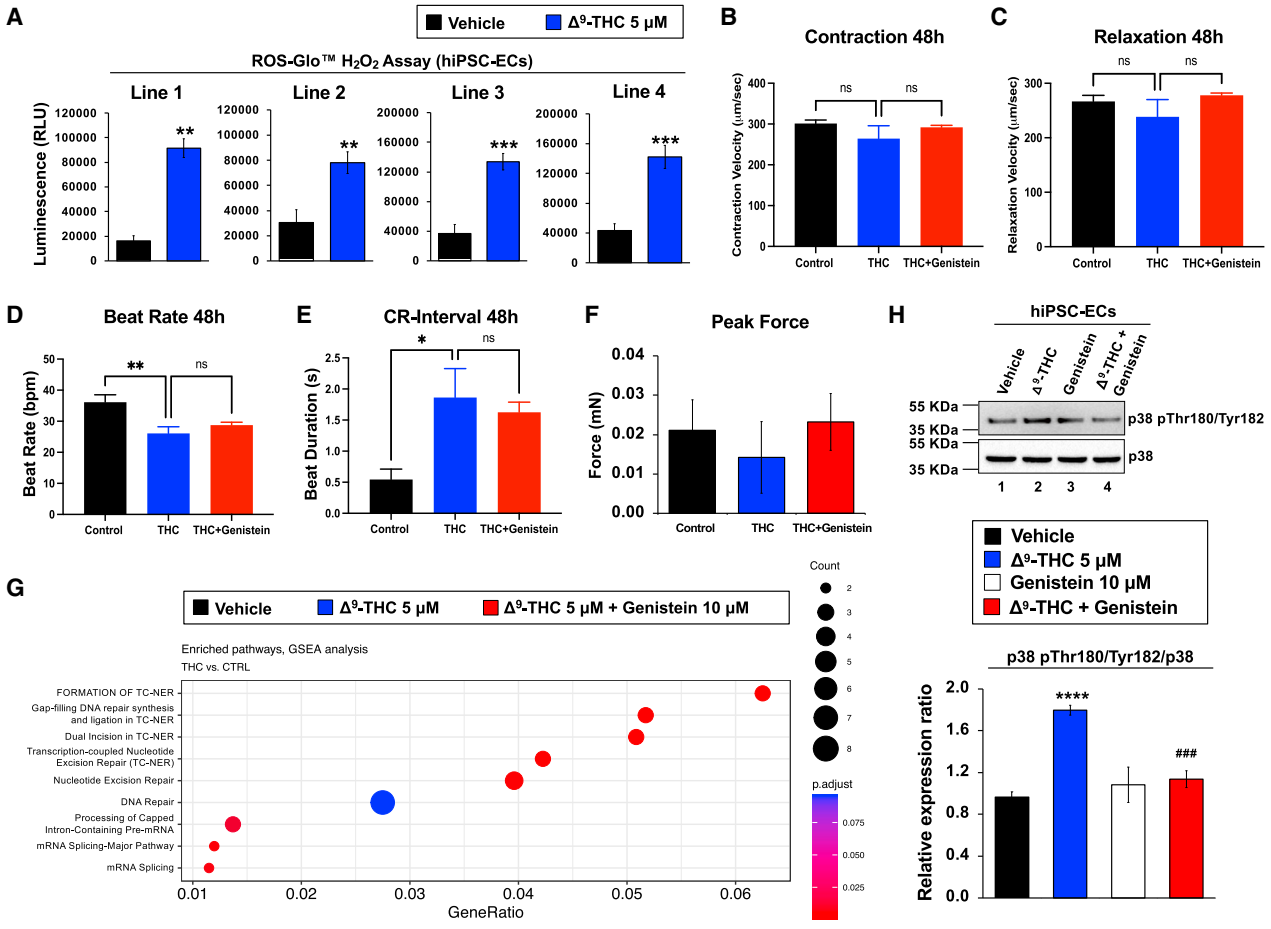

(legend on next page)

Figure S2. Assessment of Δ^9-THC effects on the expression of inflammation-related genes and oxidative stress protective-related genes in hiPSC-ECs and human-engineered heart tissues (EHTs), related to Figures 3 and 4

(A) Δ^9-THC induced hydrogen peroxide (H_2O_2) production in hiPSC-ECs. hiPSC-ECs were treated with 0.5 or 5 μM Δ^9-THC for 48 h, and ROS-Glo™ H_2O_2 assay measured the level of hydrogen peroxide.

(B) Engineered heart tissues (EHTs) were fabricated using human iPSC-derived endothelial cells and cardiomyocytes. EHTs were incubated in (1) vehicle, (2) 5 μM Δ^9-THC, or (3) 5 μM Δ^9-THC and 10 μM genistein and assayed for 48 h. After treatment exposure, EHT contractility was measured using the Sony imaging platform. There was no significant difference in EHT contractility after exposure to Δ^9-THC or cotreatment with Δ^9-THC and genistein for 48 h.

(C) EHTs showed no significant change in relaxation at 48 h with Δ^9-THC or cotreatment with Δ^9-THC and genistein.

(D) The beat rate is decreased by Δ^9-THC and not ameliorated by genistein cotreatment in EHTs.

(E) The contraction-relaxation (CR) interval was increased in EHTs after Δ^9-THC, and cotreatment with genistein did not attenuate this effect.

(F) There was no significant difference in EHT peak force at 48 h after Δ^9-THC treatment or Δ^9-THC and genistein cotreatment.

(G) Gene set enrichment analysis (GSEA) of pathways affected by Δ^9-THC treatment in EHTs. Pathways are more skewed in log fold change (logFC) distribution than expected by chance in Δ^9-THC (THC) versus vehicle control (CTRL) and are downregulated in Δ^9-THC-treated EHTs.

(H) Genistein decreased Δ^9-THC-induced p38 phosphorylation in hiPSC-ECs. Cells were treated with 5 μM Δ^9-THC, 10 μM genistein, or their combination for 48 h. Total cell lysates were subjected to western blot analysis with anti-p38 antibody and anti-p38 phospho-Thr180/Tyr182 (p38 pThr180/Tyr182) antibody. Densitometry of p38 phospho-Thr180/Tyr182 expression was normalized to pan p38 expression.

(I) Cells were treated with 5 μM Δ^9-THC, 1 μM BAY11-7082, or their combination for 48 h. The mRNA expression of inflammation-related genes in hiPSC-ECs was quantified by qPCR analysis and normalized to GAPDH. Error bars represent mean ± SEM. *$p < 0.05$ versus vehicle; **$p < 0.01$ versus vehicle; ***$p < 0.001$ versus vehicle; ****$p < 0.0001$ versus vehicle; ns, not significant versus vehicle; $^{\#}p < 0.05$ versus Δ^9-THC; $^{\#\#}p < 0.01$ versus Δ^9-THC; $^{\#\#\#}p < 0.001$ versus Δ^9-THC;$^{\#\#\#\#}p < 0.0001$ versus Δ^9-THC.; N.D., not detected for 40 cycles by qPCR.

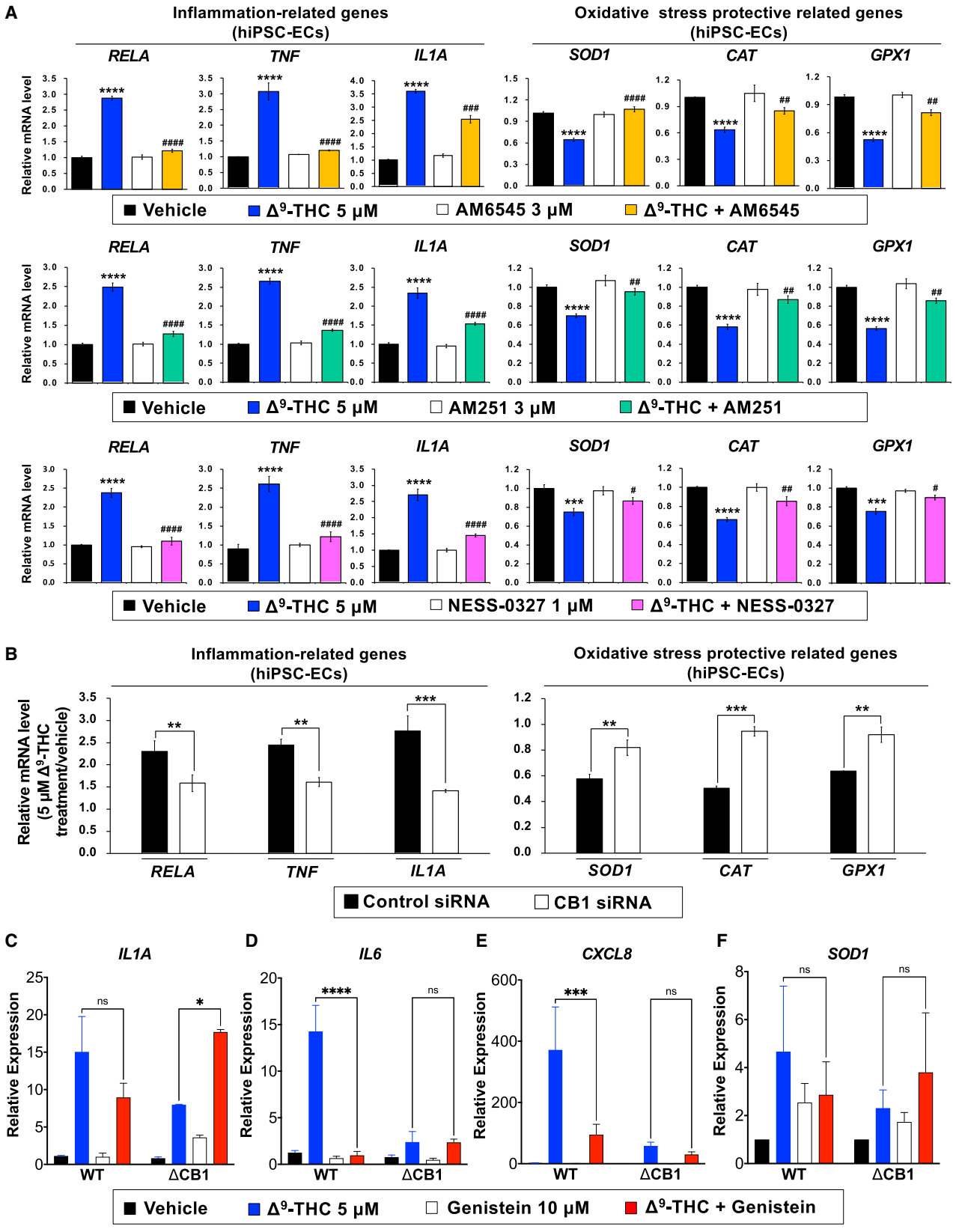

(legend on next page)

Figure S3. Inhibition of CB1 mitigates the effects of Δ^9-THC on hiPSC-ECs, related to Figure 5

(A) The selective CB1 antagonists AM6545, AM251, and NESS-0327 blocked the expression of inflammation-related genes and oxidative stress protective-related genes. Gene expression of inflammation-related genes and oxidative stress protective-related genes in hiPSC-ECs were quantified by qPCR analysis. hiPSC-ECs were treated with 5 μM Δ^9-THC and either 3 μM AM6545, 3 μM AM251, or 1 μM NESS-0327, or their combination of 5 μM Δ^9-THC and CB1 antagonist for 48 h, and the gene expression was normalized to GAPDH.

(B) The effect of siRNA-mediated knockdown of CB1 on Δ^9-THC-induced inflammation and oxidative stress in hiPSC-ECs. The hiPSC-ECs were treated with 5 μM Δ^9-THC for 48 h. The mRNA expression of inflammation-related genes and oxidative stress protective-related genes was quantified by qPCR analysis and normalized to GAPDH.

(C) Wild-type (WT) hiPSC-ECs and CRISPRi edited hiPSC-ECs were incubated with 0 or 10 ng/mL TNF-α either alone or in the presence of 10 μM genistein. The expression of *IL1A* decreased with cotreatment of TNF-α and genistein in WT hiPSC-ECs but increased significantly in CB1 CRISPRi hiPSC-ECs.

(D) The expression of *IL6* increased with TNF-α for WT and CRISPRi hiPSC-ECs but was attenuated by cotreatment with genistein in the WT hiPSC-ECs.

(E) The expression of *CXCR8* increased with TNFα for WT and CRISPRi hiPSC-ECs but was attenuated in WT hiPSC-ECs.

(F) The expression of *SOD1* increased in response to TNF-α and was not attenuated by genistein in either WT or CB1 CRISPRi hiPSC-ECs. Error bars represent mean ± SEM. *$p < 0.05$ versus vehicle; **$p < 0.01$ versus vehicle; ***$p < 0.001$ versus vehicle; ****$p < 0.0001$ versus vehicle; ns, not significant versus vehicle; #$p < 0.05$ versus Δ^9-THC; ##$p < 0.01$ versus Δ^9-THC; ###$p < 0.001$ versus Δ^9-THC; ####$p < 0.0001$ versus Δ^9-THC.

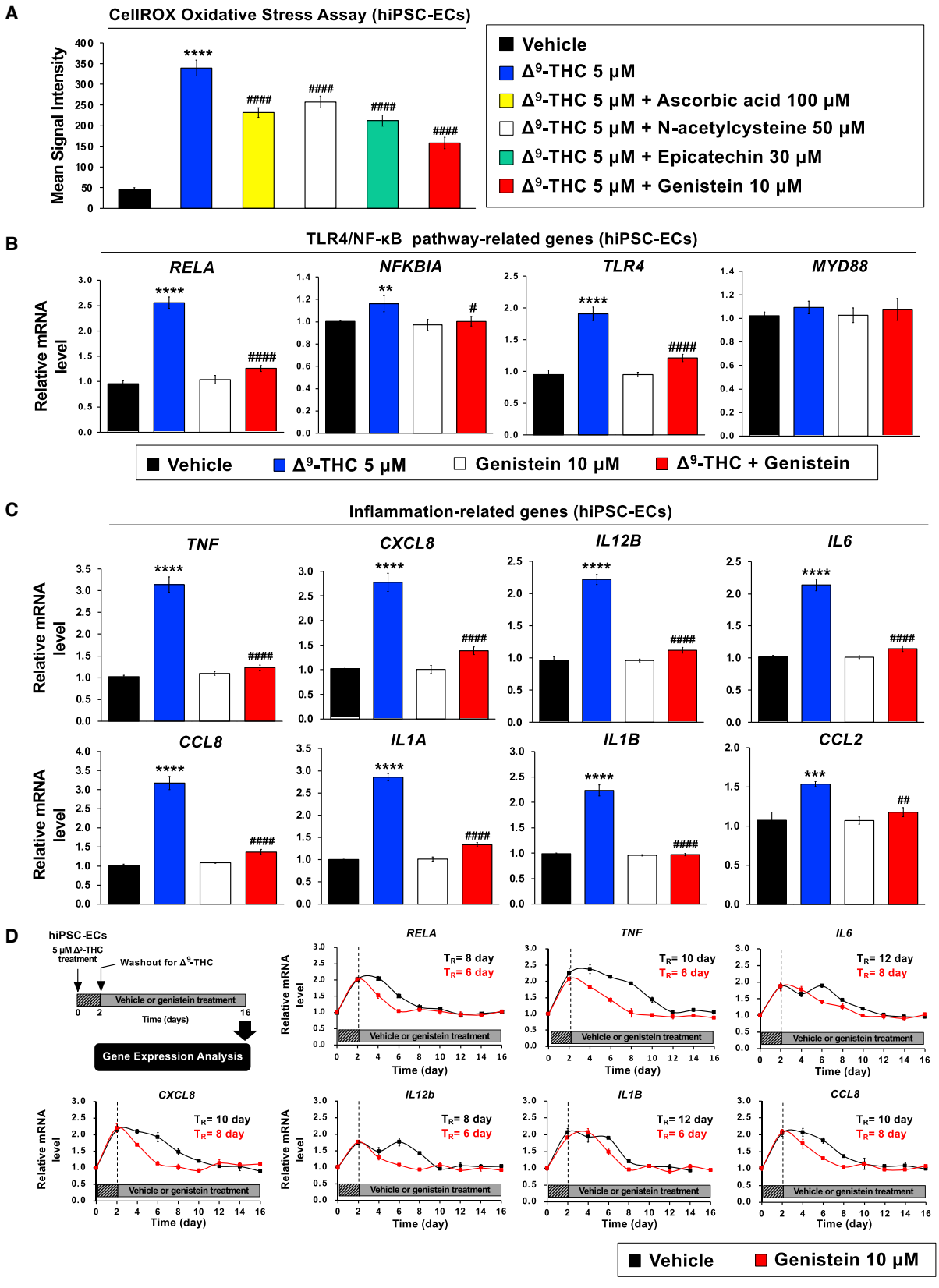

(legend on next page)

Figure S4. Assessment of the effects of antioxidants on Δ^9-THC-induced oxidative stress and inflammation in hiPSC-ECs, related to Figure 5

(A) hiPSC-ECs were treated with 5 μM Δ^9-THC and various antioxidant reagents for 48 h, and CellROX oxidative stress assay measured the level of oxidative stress.

(B) Genistein attenuated the effects of Δ^9-THC on TLR4/NF-κβ-related genes. Cells were treated with 5 μM Δ^9-THC, 10 μM genistein, or a combination of both for 48 h, and the mRNA expressions of TLR4/NF-κβ-related genes were measured by qPCR analysis. The levels of mRNA were normalized to GAPDH.

(C) Genistein prevented Δ^9-THC-mediated inflammation-related genes in hiPSC-ECs.

(D) Genistein attenuated Δ^9-THC-induced inflammation in hiPSC-ECs. The cells were treated with 5 μM Δ^9-THC for 48 h, then replaced with fresh cell culture medium, and 10 μM genistein was added. Total RNA was isolated from hiPSC-ECs every other day for 2 weeks. The mRNA expression of inflammation-related genes was quantified by qPCR and normalized to GAPDH. The retention time (T_R) is the time required to recover gene expression to the basal level. Error bars represent mean ± SEM. *$p < 0.05$ versus vehicle; **$p < 0.01$ versus vehicle; ***$p < 0.001$ versus vehicle; ****$p < 0.0001$ versus vehicle; ns, not significant versus vehicle; $^{\#\#}p < 0.01$ versus Δ^9-THC; $^{\#\#\#}p < 0.001$ versus Δ^9-THC; $^{\#\#\#\#}p < 0.0001$ versus Δ^9-THC.

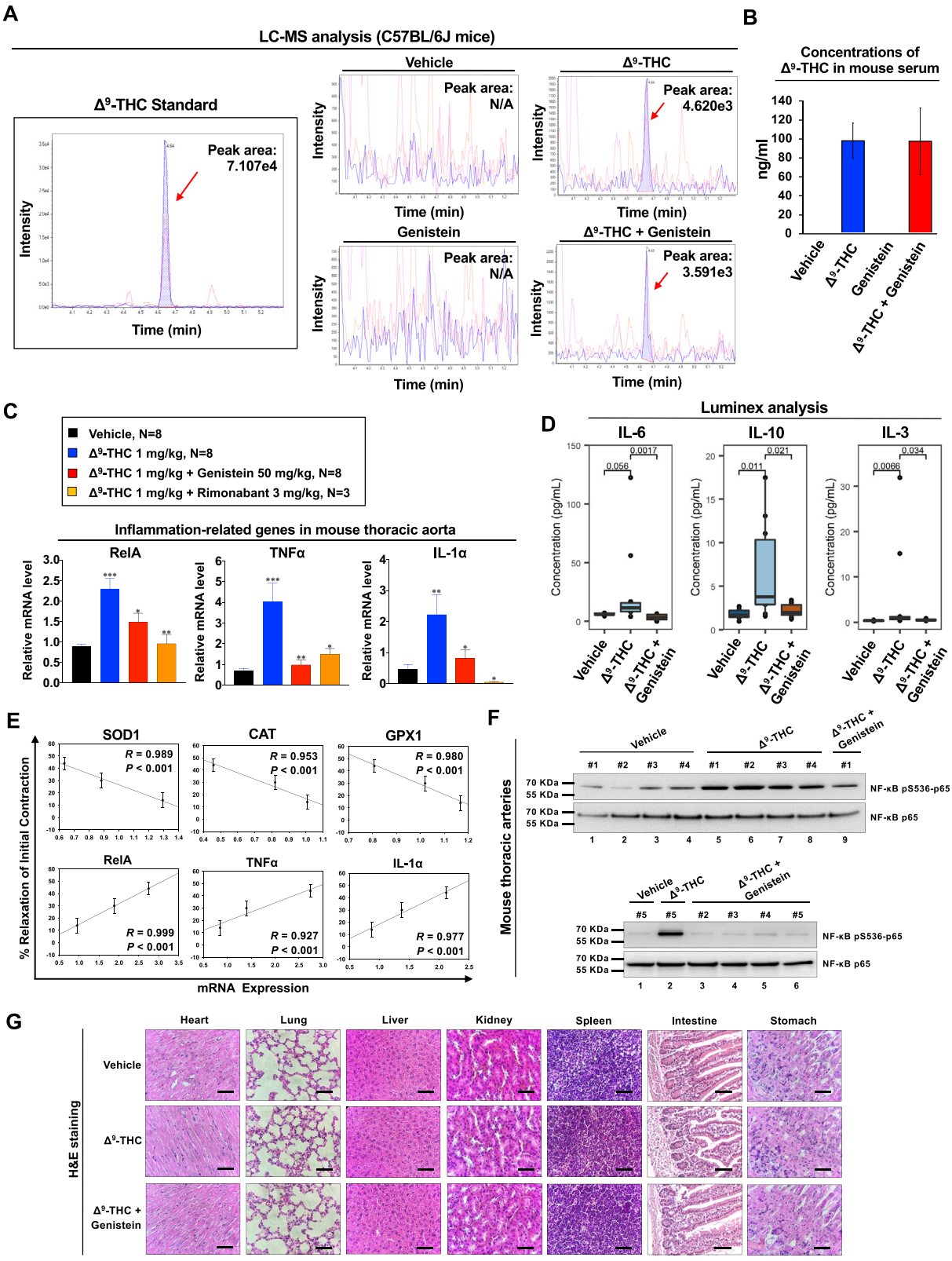

(legend on next page)

Figure S5. Assessment of the effects of genistein on Δ^9-THC-induced effects in C57BL/6J mouse model, related to Figure 6

(A) Liquid chromatography and mass spectrometry (LC-MS) analysis of mouse plasma with the reference standard for Δ^9-THC is shown. Male C57BL/6J mice were treated with (1) vehicle control, (2) genistein, (3) Δ^9-THC, or (4) Δ^9-THC plus genistein (n = 5/group). All mice were sacrificed after 30 days, and plasma was isolated using 5 mM EDTA. Isolation of Δ^9-THC (retention time [tR] ≈ 4.64 min) was performed by LC analysis. The desired fraction (tR ≈ 4.64 min) was collected and subjected to the MS analysis.

(B) Δ^9-THC concentration (ng/mL) of mouse plasma was measured by the LC-MS analysis for each treatment group.

(C) The mRNA expression of inflammation-related genes and oxidative stress protective-related genes. The C57BL/6J mice (n = 5/group) were treated with (1) vehicle control, genistein, (2) Δ^9-THC, (3) Δ^9-THC plus genistein, or (4) Δ^9-THC plus rimonabant.

(D) Luminex analysis of inflammatory cytokines in plasma of C57BL/6J mice treated with vehicle control, Δ^9-THC, or Δ^9-THC plus genistein. IL-6, IL-10, and IL-3 levels were elevated after treatment with Δ^9-THC. Genistein cotreatment significantly reduced the expression of these cytokines (p values are shown).

(E) Arterial relaxation is correlated with the expression of oxidative stress protective-related genes and inflammation-related genes.

(F) The effect of Δ^9-THC on NF-κB phosphorylation in mouse thoracic artery tissues (n = 5). Total cell lysates were prepared, and the expressions of NF-κB, phosphorylated NF-κB, and β-actin were analyzed by western blot analysis.

(G) Three sections of each organ were counterstained with H&E, and one representative slide was presented. Scale bars, 250 μm.

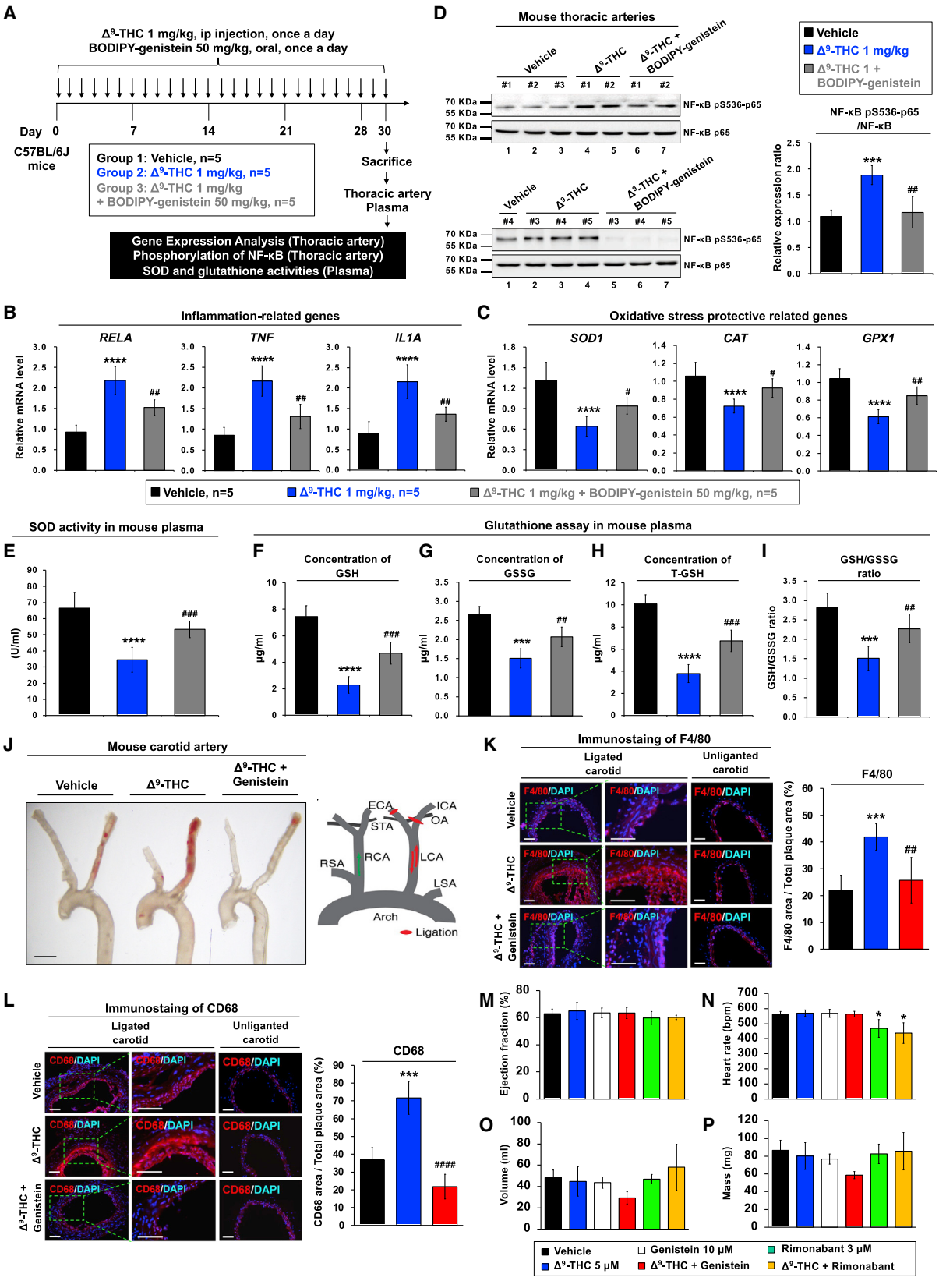

(legend on next page)

Figure S6. Assessment of the effects of BODIPY-genistein and genistein on Δ^9-THC-induced effects in multiple mouse models, related to Figures 6 and 7

(A) BODIPY-genistein blocked Δ^9-THC-induced inflammation and oxidative stress *in vivo*. Schematic overview of the experimental design in the mouse model.
(B and C) (B) The mRNA expression of inflammation-related genes and (C) oxidative stress protective-related genes in thoracic artery tissues from mice is shown after normalizing to GAPDH.
(D) Δ^9-THC increased and BODIPY-genistein attenuated NF-κB phosphorylation in mouse thoracic artery. Total cell lysates were prepared, and the expression of phosphorylated NF-κB and NF-κB was analyzed by western blot analysis (left panel). Immunoblots were quantified by ImageJ software (right panel).
(E) Superoxide dismutase (SOD) activity of serum from the mouse.
(F) Reduced glutathione (GSH) levels in the serum samples of mice were detected. Plasma isolated from C57BL/6J mice treated with (1) vehicle control, (2) Δ^9-THC, or (3) Δ^9-THC plus BODIPY-genistein every day for 30 days and were analyzed by the glutathione colorimetric assay kit (BioVision, K261).
(G) Oxidized glutathione (GSSG) levels in the serum samples of mice.
(H) Total glutathione (T-GSH) levels in the serum samples of mice.
(I) The GSH/GSSG ratio in the serum samples of mice.
(J) Gross images of carotid arteries after oil red O staining are shown (left panel). The scale bar represents 1 mm. A diagram of partial ligation of the carotid artery is shown (right panel). The left common carotid artery (LCA), external carotid artery (ECA), internal carotid artery (ICA), and superior thyroid artery (STA) were ligated, leaving the occipital artery (OA) open. The right subclavian artery (RSA), right common carotid artery (RCA), and left subclavian artery (LSA) were unligated and remained patent.
(K) Carotid artery sections were immunostained with an anti-F4/80 antibody, and one representative experiment was presented. High-magnification images of the green-boxed area are shown. The scale bar represents 250 μm. Quantification of F4/80-positive area within carotid artery sections.
(L) Carotid artery sections were immunostained with an anti-CD68 antibody, and one representative experiment was presented. High-magnification images of the green-boxed area are shown with the scale bar at 250 μm. Quantification of CD68-positive area within carotid artery sections is shown.
(M) Left ventricular systolic function is normal in C57BL/6J treated with vehicle control, Δ^9-THC (1 mg/kg i.p.); genistein (50 mg/kg p.o.); Δ^9-THC (1 mg/kg i.p.) and genistein (50 mg/kg p.o.); rimonabant (3 mg/kg p.o.); or rimonabant (3 mg/kg p.o.) and Δ^9-THC (1 mg/kg i.p.). Mice were anesthetized with 1%–2% isoflurane, and images were acquired in the parasternal long-axis (PLA) and parasternal short axis (PSA) on a Visualsonic Vevo 2100 platform. The ventricular (LV) dimensions were traced offline, and the ejection fraction (EF) was calculated using Simpson's biplane method of discs.
(N) The heart rate measured at the time of echocardiography did not vary between vehicle, genistein, Δ^9-THC, or Δ^9-THC plus genistein.
(O) Left ventricular end-diastolic volume (LVEDV) of mice did not significantly differ in either treatment group.
(P) Left ventricular end-diastolic mass (LVEDM) of mice treated was comparable similar among treatment groups. Error bars represent mean ± SEM. *$p < 0.05$ versus vehicle; **$p < 0.01$ versus vehicle; ***$p < 0.001$ versus vehicle; ****$p < 0.0001$ versus vehicle; ns, not significant versus vehicle; #$p < 0.05$ versus Δ^9-THC; ##$p < 0.01$ versus Δ^9-THC; ###$p < 0.001$ versus Δ^9-THC; ####$p < 0.0001$ versus Δ^9-THC.

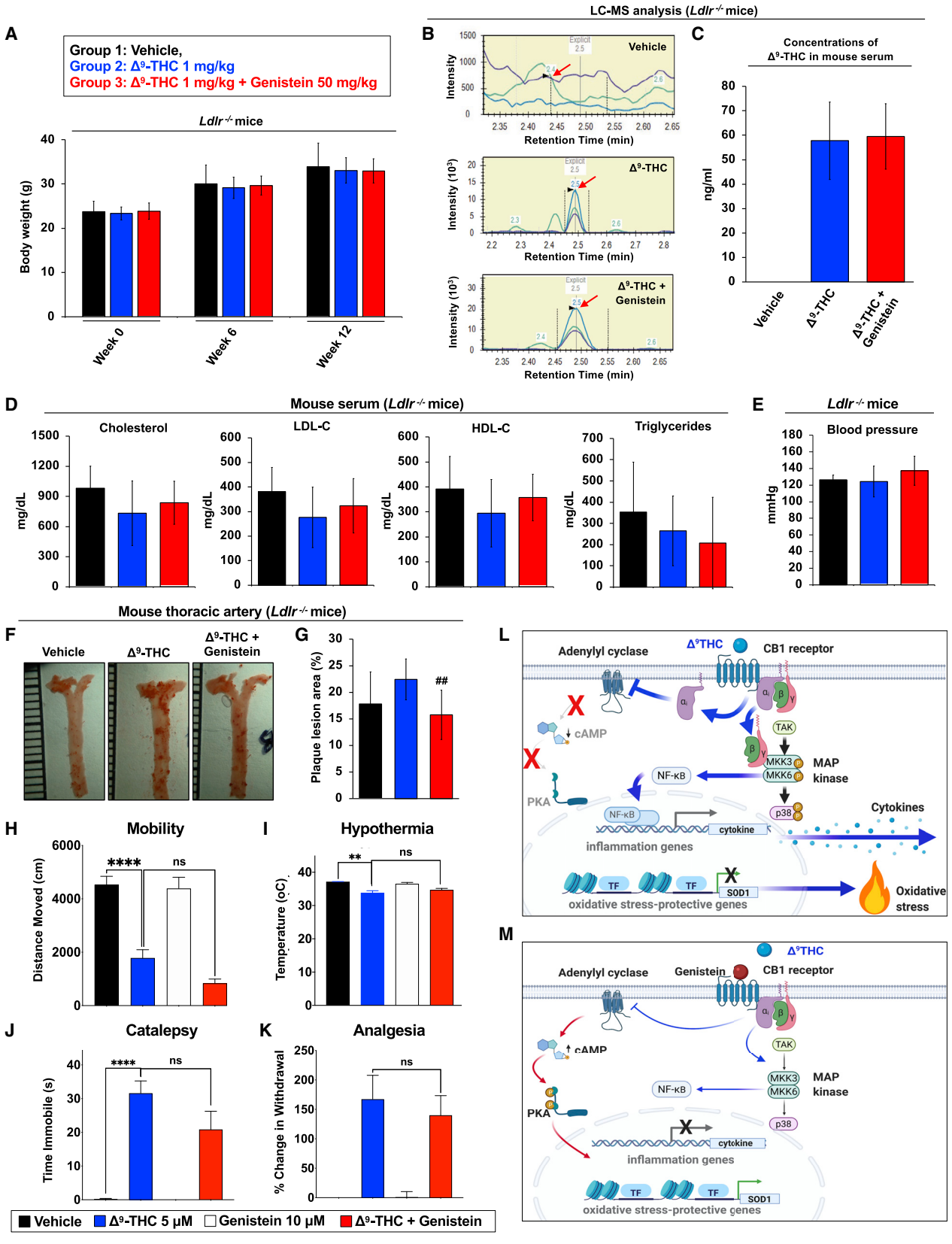

(legend on next page)

Figure S7. The *Ldlr*$^{-/-}$ mouse model of atherosclerosis and *in vivo* neurobehavioral testing for the CB1 antagonist genistein, related to Figures 6 and 7

(A) The body weights of *Ldlr*$^{-/-}$ mice after exposure to (1) vehicle control (n = 10), (2) Δ^9-THC (n = 12), or (3) Δ^9-THC plus genistein (n = 12).

(B and C) Serum concentration of Δ^9-THC in *Ldlr*$^{-/-}$ mice measured by LC-MS analysis for *Ldlr*$^{-/-}$ mice after exposure to (1) vehicle control (n = 7;) [B], upper panel), (2) Δ^9-THC (n = 7; [B], middle panel), or (3) Δ^9-THC plus genistein (n = 8; [B], lower panel). Quantification of Δ^9-THC in *Ldlr*$^{-/-}$ mice by LC-MS analysis (C).

(D) Lipid profiles of serum samples of *Ldlr*$^{-/-}$ mice at 12 weeks after mice after exposure to (1) vehicle control (n = 10), (2) Δ^9-THC (n = 12), or (3) Δ^9-THC plus genistein (n = 12).

(E) The blood pressure of Ldlr$^{-/-}$ mice after exposure to (1) vehicle control (n = 3), (2) Δ^9-THC (n = 4), or (3) Δ^9-THC plus genistein (n = 4) for 30 days measured by tail-cuff.

(F) Gross images of oil red O stained *Ldlr*$^{-/-}$ thoracic aorta are shown.

(G) Quantification of plaque size by *en face* analysis of thoracic aorta after exposure to (1) vehicle control (n = 10), (2) Δ^9-THC (n = 12), or (3) Δ^9-THC plus genistein (n = 12).

(H) Spontaneous activity was impaired by Δ^9-THC and not attenuated by genistein. C57BL/6J mice were exposed to (1) vehicle control (intraperitoneal [i.p.], vehicle and oral [p.o.], vehicle [n = 8]), (2) Δ^9-THC at 20 mg/kg i.p. and p.o. vehicle (n = 9), (3) genistein at 50 mg/kg p.o. and i.p. vehicle (n = 8), and (4) combination of Δ^9-THC at 20 mg/kg i.p. and genistein at 50 mg/kg p.o. (n = 9). Spontaneous activity was assessed by the total distance moved in an activity chamber and was reduced with Δ^9-THC treatment. Genistein did not affect distance moved either alone or in combination with Δ^9-THC.

(I) Genistein did not affect hypothermia induced by Δ^9-THC. Hypothermia was assessed by measuring body temperature using a rectal probe before and 60 min after treatment. Δ^9-THC caused a significant decrease in temperature, and genistein did not affect temperature and could not ameliorate hypothermia induced by Δ^9-THC.

(J) Genistein did not impair catalepsy after Δ^9-THC treatment. The bar test measures the time a mouse remained immobile on the bar. Pre-exposure time showed no differences between groups. However, mice treated with Δ^9-THC remained immobile longer than control, and genistein did not improve immobility.

(K) Analgesia induced by Δ^9-THC is not affected by genistein cotreatment. Analgesia was measured by placing mice on a hot plate and recording the time for the mouse to withdraw or lick. Mice treated with Δ^9-THC had greater withdrawal or lick latency than control or genistein treatment. Genistein cotreatment did not affect Δ^9-THC mediated analgesia.

(L) Schematic of Δ^9-THC-induced endothelial dysfunction. Δ^9-THC causes endothelial dysfunction with the induction of inflammation and oxidative stress. Δ^9-THC activates the CB1 receptor and causes inhibition of adenylyl cyclase, which reduces cAMP levels and protein kinase A (PKA) phosphorylation, and thus, Δ^9-THC-binding inactivates gene expression via PKA. Δ^9-THC also increases phosphorylation of MAP kinase and translocation of NF-$\kappa\beta$ to the nucleus. Hence, Δ^9 -THC-binding activates the expression of inflammation-related genes and inhibits the expression of oxidative stress protective-related genes.

(M) Schematic of genistein attenuating Δ^9-THC-induced endothelial dysfunction. Genistein, a soybean flavonoid, can attenuate Δ^9-THC-induced side effects *in vitro* and *in vivo*. Genistein occupies the same binding site at Δ^9-THC and is a neutral antagonist for the CB1 receptor. Genistein binding does not affect downstream signaling but prevents Δ^9-THC binding, thus preventing activation of genes implicated in inflammation and repression of oxidative stress protective genes. Created with BioRender.com.